Local metal to non-metal transition on oxygen-covered platinum particles from ^{195}Pt nuclear magnetic resonance

1995 J. Phys.: Condens. Matter 7 2447

(http://iopscience.iop.org/0953-8984/7/12/009)

J. Phys.: Condens. Matter 7 (1995) 2447–2459. Printed in the UK

Local metal to non-metal transition on oxygen-covered platinum particles from ^{195}Pt nuclear magnetic resonance

Y Y Tong and J J van der Klink
Institut de Physique Expérimentale, Ecole Polytechnique Fédérale de Lausanne, CH-1015 Lausanne, Switzerland

Received 27 September 1994, in final form 14 November 1994

Abstract. The nuclear magnetic resonance (NMR) parameters (shift, relaxation time) in a metal are determined by the Fermi-level local density of states (LDOS), and the nuclear spin–lattice relaxation rate is proportional to the temperature (Korringa relation). In the ^{195}Pt NMR spectrum of platinum catalysts, signals from surface atoms and from atoms deeper in the particles can be distinguished; furthermore the NMR parameters are sensitive to the chemisorption of gases (oxygen in the present case). Using the Korringa relation as the criterion, we find that at moderate oxygen coverage (O/surface Pt ratios of 0.16 and 0.40) part of the surface atoms are non-metallic (have zero LDOS), while at zero or at saturation coverage (O/surface Pt = 0.75) all atoms show metallic behaviour. In addition, some possible relations between NMR-derived variations of the LDOS and chemisorption properties are indicated.

1. Introduction

In a frontier-orbital picture of bonding to metal surfaces, the states near the Fermi energy E_F play the role of the highest occupied and lowest unoccupied orbitals in molecular bonding (for a review see [1]). Since electrons with energy close to E_F can be rearranged at low energetic cost, they are thought to be important for the initial interaction between an incoming reactant molecule and the metal surface. One may therefore expect a relation between the reactivity of a surface and the Fermi-level local densities of states (LDOS) on the surface sites. In principle, metal nuclear magnetic resonance (NMR) measures these quantities without perturbing the electronic structure of the surface (the quanta of NMR have energies of a fraction of a kelvin). In practice some modelling is necessary to go from the experimental quantities (Knight shift and spin–lattice relaxation time) to the desired densities of states [2, 3]. For the interpretation of NMR data in transition metals, it is usual to suppose that separate s-like and d-like densities of states and their associated hyperfine fields can be distinguished [3, 4]. When there is a site-to-site variation in the NMR parameters K (Knight shift) and T_1 (nuclear spin–lattice relaxation time), such as occurs in ^{195}Pt NMR of catalysts [2, 5], this is ascribed to a variation in the s-like and d-like LDOS at the Fermi level; all other quantities in the equations for K and T_1 are considered site-independent. The latter assumption is not necessarily completely correct: therefore the actual values found this way must be treated with some caution, but it is thought that the trends (increasing or decreasing values; widening or narrowing of the distribution of values) are correct [2, 6, 7].

Ideally, the contribution of metal NMR to our knowledge of platinum catalysts would consist of the determination of a complete distribution curve of the s-like and d-like LDOS over the ensemble of atomic sites in the sample; by varying the particle size distribution somewhat from one sample to another, one might hope to identify what parts of the LDOS

0953-8984/95/122447+13$19.50

distribution curves correspond to what geometrical kind of site (volume, surface, edge, corner, etc). As a first step towards this goal, we have supposed in earlier work [8] that the principal characteristic of a site is the 'layer' (surface layer, subsurface layer, and so on) in which it is situated. The fraction of atoms in each layer is determined from particle size histograms obtained by electron microscopy and from theoretical layer statistics for cubooctahedral particles. The distribution of LDOS values over the different atoms in a given layer is then characterized by an average (or a 'typical') value and by its width. As an example, the data in figure 6 of the paper by Bucher *et al* [8] indicate that the clean surface sites in their sample have a total LDOS distribution of width 3.3 and average 14.8 states per Rydberg per atom; saturation coverage with hydrogen changes the width to 5.1 and the average value to 11 in the same units. (The LDOS distribution widens upon hydrogen chemisorption, although the width of the NMR surface peak diminishes.)

In metal NMR, we call two nuclear sites 'similar' only when they give rise to both the same Knight shift and the same nuclear spin–lattice relaxation time; this means that both the s-like and the d-like LDOS at the Fermi level must be the same. (In a more general sense, two sites are 'identical' only when the full spectrum of LDOS is the same; but NMR gives only information on a small region of that spectrum, of width approximately kT around the Fermi energy.) In the case of clean platinum particles on oxidic supports (we have mostly used titania, but silica and alumina do not seem to give other results) the analysis in terms of s-like and d-like LDOS indicates that the s-like LDOS varies but little from one site to another [2]. As a consequence, only the d-like LDOS determines whether two sites are different; the Knight shift and the relaxation time change simultaneously. Therefore, all nuclei that resonate at a given frequency have the same T_1, and the experimental relaxation curves are simple exponentials. In the more general case, many combinations of s-like and d-like LDOS may result in exactly the same Knight shift, but different relaxation times. This superposition of several spin–lattice relaxation curves can result in visibly non-exponential behaviour. The Korringa relaxation in metals is easily identified by its characteristic temperature dependence: the relaxation rate is proportional to the temperature. For multiple-exponential relaxation, this means that relaxation curves obtained at different temperatures must collapse into a single plot by scaling the time axis with the temperature (time/temperature scaling) [6].

In the data on oxygen chemisorption that we present in this paper, an additional complication arises: we find non-exponential relaxation that under some circumstances is only partly due to the Korringa mechanism. This implies that on a part of the atoms in the sample, the local density of states at the Fermi level is zero (or very low) and that their Knight shift must be zero as well (so that the observed shifts are chemical shifts): these atoms are in a non-metallic environment. We will argue that they are situated on the surface, and that there are both non-metallic and metallic surface atoms. As before, the distribution of LDOS values on the metallic surface sites will be characterized by specifying a width and an average value, both derived from the Korringa-like part of the relaxation curves taken at different positions in the surface region of the spectrum.

2. Experimental methods

The starting platinum catalyst to prepare our NMR samples is from the same batch as sample 3 in [9]. It is 4.4 wt.% Pt on TiO_2-anatase and was synthesized by an ion-exchange method. The dispersion, determined by transmission electron microscopy (TEM), is 60%, corresponding to an average particle size of 1.7 nm. Oxygen dosing was calculated from

the chemisorption isotherm of oxygen at room temperature. The sample was first cleaned by hydrogen at 300 °C and then evacuated at 430 °C for ca. 5 h. Oxygen was admitted to the sample cell with a controlled pressure at room temperature. The quantity taken up was determined by the usual volumetric method. After oxygen dosing, the cell was evacuated at room temperature for ca. 1.5 to 2.0 h (the final vacuum reached ca. 8.0×10^{-6} mbar), and the sample was sealed immediately in a glass ampoule under He atmosphere (about 400 Torr) without further contact with air. Three samples with oxygen coverages in terms of (O atoms/(surface Pt atoms) of 0.16, 0.40 and 0.75 were so prepared, designated as Pt-60-O16, Pt-60-O40 and Pt-60-O75 respectively. For Pt-60-O75, the sample has been left in ca. 1 bar of oxygen for 120 h at room temperature before the final evacuation.

From x-ray studies on the standard Pt/SiO_2 catalyst EuroPt-1 [10], it has been concluded that an important fraction of the oxides in the as-received catalyst is PtO. This compound has recently been obtained in bulk form and is thought to be a p-type semiconductor [11]. In a Raman spectroscopic study of a γ-alumina-supported catalyst the major oxide has been identified as α-PtO_2 [11, 12]; the latter compound is easily available. The x-ray spectra of a powder obtained from the Aldrich Chemical Co. have been reported [11] to agree well with those from sputtered films. We used a powder from that same source for comparative NMR measurements.

All NMR spectra were taken point-by-point by scanning the frequency with a spin-echo method ($\pi/2$–τ–π–τ–echo). The length of $\pi/2$ pulse varied from about 4.6 to 8 μs, depending on the spectrometer, the probehead used and other experimental details. The value of τ was always 20 μs. The spin–lattice relaxation time was measured by recording the recovery of spin-echo intensity after a saturation pulse-comb (seven $\pi/2$ pulses followed by $(\pi/4)_{-y}(\pi/2)_{+x}(\pi/2)_{+y}(\pi/4)_{+x}$ [13], with gradually reduced time intervals between the pulses).

The nuclear spin–lattice relaxation measured in the low-field spectral region is non-exponential, and can be represented by a five-parameter double-exponential function. The five parameters were determined by a non-linear least-squares fit. To obtain an estimate of the uncertainty in each of the parameters, N additional pseudo-data sets were constructed from the original one by adding random 'noise' to each of the measured amplitudes. The amplitude of the added noise was chosen on the basis of the standard deviation in the initial fit. Next the fitting procedure was repeated for each of the N artificial data sets, and the standard deviation of the parameters in these N fits was taken as the estimate of their uncertainty. Typically, a full relaxation curve consisted of 20 experimental points, and the number $N = 8$. The uncertainties determined this way were usually of the order of 10%. Generally, the procedure was performed twice: once using the amplitude of the spin-echo, and once using its integral. In nearly all cases, the two sets of data agreed within the 10% limit. Where this was not the case, the difference between the two sets has been used as error estimate.

Since the experimental Knight shift is known very precisely, the main source of uncertainty in resolving the equations comes from T_1. The densities of state appear as quadratics in equation (2) (see below), and therefore the typical error of 10% in the spin–lattice relaxation leads to an uncertainty of 5% in the densities of state. The 'real' local densities of state may of course be different from the ones calculated here by more than that amount, because of approximations inherent in equations (1)–(2) and the hypothesis that values of the fixed parameters, determined for bulk platinum, are also valid and site-independent in small particles. As stated in section 1, we think that the trends in the changes of densities of state are correct, but that the absolute values must be treated with some caution.

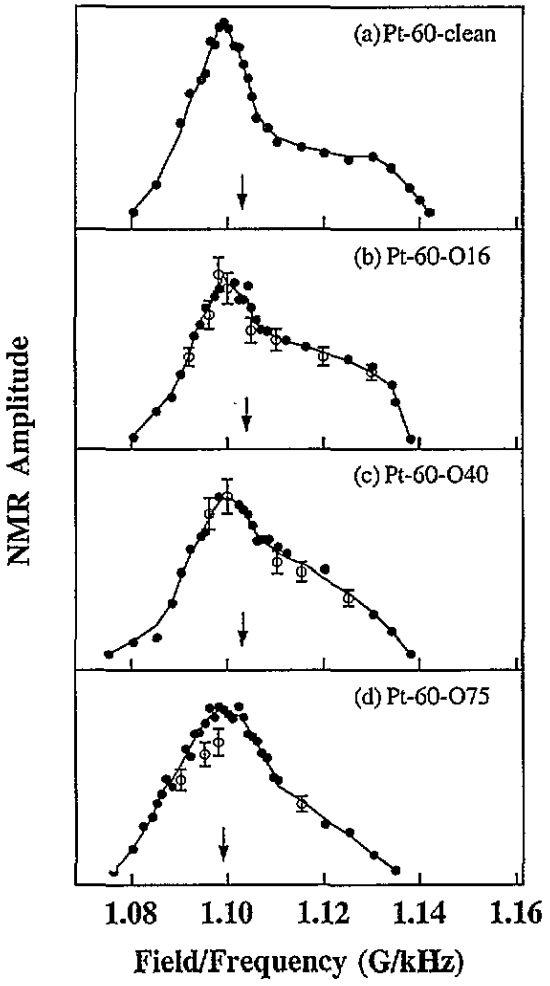

Figure 1. ^{195}Pt NMR spectra of Pt/TiO_2 catalysts measured at 80 K by the point-by-point spin-echo method. The repetition rate is 33.3 s^{-1} and the time between $\pi/2$ and π pulses is 20 μs. The spectra are not corrected for T_2 effects, and are normalized to the same area. The ratio (O atom)/(surface Pt atom) is 0, 0.16, 0.40 and 0.75 going from (a) to (d). The first moments of the spectra are indicated by arrows. The open symbols with error bars represent some points of the ^{195}Pt NMR spectra at 22 K, obtained from fits to spin–lattice relaxation data. They are scaled at the rightmost point. There seems to be no detectable change when going from 80 K to 22 K.

3. Experimental results

The ^{195}Pt NMR spectra of the clean-surface sample and the three oxygen-dosed samples have been measured at 80 K and are shown in figure 1. The centre of gravity of the spectrum shifts from 1.103 G kHz^{-1} (Pt-60-clean) to 1.104, 1.103 and 1.099 G kHz^{-1} (Pt-60-O75), and the position of the spectral maximum is not markedly affected. The surface-like NMR signal tends to broaden, and the high-field signal diminishes in amplitude with increasing oxygen coverage. Some additional spectral information can be derived from relaxation data at 22 K (see below). The equilibrium amplitudes obtained from the fits of the relaxation curves at several frequencies are plotted also in figure 1 (open symbols with error bars). The

scale of the latter has been adjusted to the highest-field point obtained from the relaxation curves. It is seen that there is no marked temperature dependence of the spectra.

On each of the three oxygen-covered samples, two types of spin–lattice relaxation experiments were done: one at constant temperature (22 K) for several frequencies within the spectrum, the other at fixed frequency and variable temperature. At 22 K, the relaxation curves of the high-field signals (field/frequency ratios greater than or equal to 1.115 G kHz^{-1}) are single-exponential and the values of the relaxation times are almost independent of surface treatment: therefore this part of the spectrum is due to atoms in the interior of the particles. Assuming that the geometrical layer statistics are not changed by the chemisorption, all samples have 60% of the atoms in the surface layer, 29% in the subsurface layer and 11% in the deeper layers. The fraction of the NMR signal above 1.115 G kHz^{-1} changes with increasing dosing of oxygen from 0.31 (Pt-60-clean) to 0.34, 0.30 and 0.19 (Pt-60-O75). The differences in the first three numbers are hardly significant, and the last value shows that even at saturation coverage the influence of oxygen goes less deep than that of hydrogen [6].

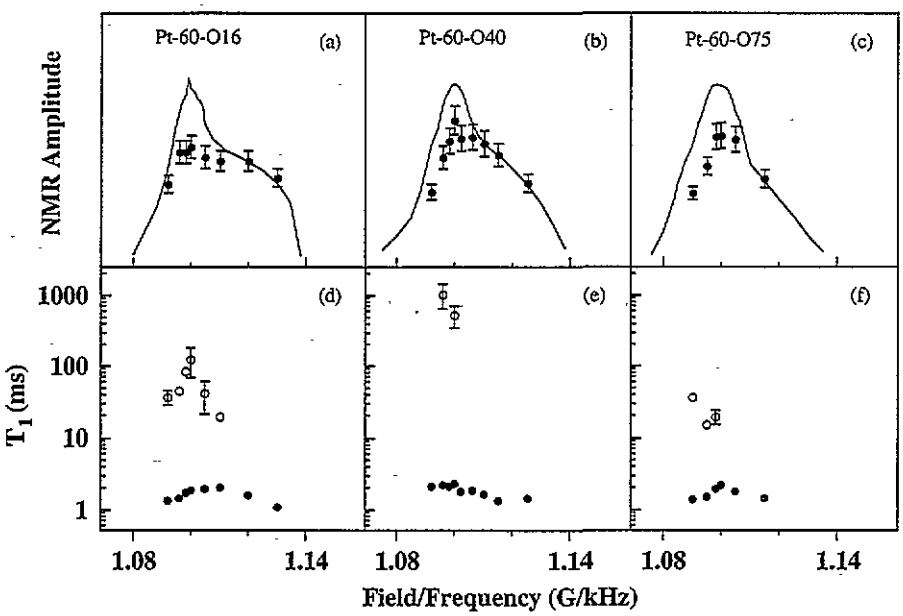

Figure 2. Spin–lattice relaxation data at 22 K for several positions in the spectra, fitted to double exponentials for $H_0/\nu_0 < 1.115$ G kHz^{-1} and to single exponentials in the other points. Top row: amplitude of the faster exponential (points) and fully relaxed spectra (full curve). Bottom row: relaxation times of the faster (full symbols) and of the slower (open symbols) exponentials. The oxygen coverage is 0.16, 0.40 and 0.75 going from left to right.

In the low-field part of the spectra (still at 22 K), the relaxation curves are multiple-exponential, and different from sample to sample. They can all be fitted to double exponentials (at some frequencies full relaxation curves have been measured, yielding both slow and fast components; at others only the fast component has been observed). The relative amplitude of the two exponentials is shown in figure 2 (top row), and the corresponding relaxation rates in figure 2 (bottom row). The choice of a double exponential (rather than triple or quadrupole, or than a continuous distribution of relaxation times) is

mostly one of convenience; we certainly do not think that there are exactly two different types of atoms resonating at the same frequency. As will be discussed below, the fixed-frequency, variable-temperature experiment shows that in Pt-60-O16 and Pt-60-O40 the faster of the exponentials follows the Korringa relation, while the other does not. Therefore we suppose for these two samples that everywhere in the surface region of the spectrum the two exponentials are due to two distinct groups of nuclei: those in a metallic, and those in a non-metallic environment. The fractions of non-metallic atoms estimated from figure 2(a) and (b) are collected in table 1. If we assume all non-metallic nuclei to be in the surface, the number of slowly relaxing Pt nuclei per oxygen atom decreases from 2.7 (O16) to 1.5 (O40). In Pt-60-O75, the double-exponential relaxation will be interpreted as indicating a range of (rather than exactly two) metallic sites with different LDOS, in the same way as was done earlier for hydrogen-covered samples [6]. The width of the LDOS distribution is indicated by the differences in the LDOS derived from the 'fast' and from the 'slow' relaxation times, whereas the average is obtained by weighing these LDOS with the relative amplitudes of the rapidly and the slowly relaxing exponentials.

The variable-temperature experiments on Pt-60-O16, −O40 and −O75 were performed at fixed frequencies corresponding to respectively 1.098, 1.100 and 1.095 G kHz^{-1}. As demonstrated by time/temperature scaled plots (not shown), part of the signal in the first two cases relaxes in a non-Korringa way. All curves can be fitted to double exponentials, with temperature-independent ratios of the faster- and slower-relaxing contribution (see caption of figure 3 for detailed values). The relaxation rates found from the fits are shown as a function of temperature in doubly logarithmic plots in figure 3. The lack of time/temperature scaling for some of the signal means that on some atomic sites the density of Fermi-level electrons is zero (or very low).

The NMR spectrum obtained on α-PtO_2 (not shown) peaks at 1.089 G kHz^{-1} and compares well with earlier spectra [8]. In figure 4, a series of time/temperature scaled relaxation curves is presented. The scaling, however, is with a factor T^2, characteristic of relaxation by phonon scattering (Raman relaxation) in insulators, instead of a factor T, as in metals. While it is not easy to identify the relaxation mechanism, the result shows clearly that the NMR of the surface oxides in the samples studied here does not resemble that of α-PtO_2.

4. Interpretation of data

For nuclei in a metallic environment, the combined information on resonance frequency (expressed as Knight shift K) and on relaxation (expressed as the Korringa product T_1T, where T is temperature and T_1 one of the two spin–lattice relaxation times found from the fit) is used to find the local s-like and d-like densities of state $D_s(E_F)$ and $D_d(E_F)$ from the equations [2]:

$$K = [1/(1-\alpha_s)]\mu_B^2 D_s(E_F)H_{hf,s} + [1/(1-\alpha_d)]\mu_B^2 D_d(E_F)H_{hf,d} + \chi_{orb}H_{hf,orb}/\mu_B$$
$$= K_s + K_d + K_{orb} \tag{1}$$

$$S(T_1T)^{-1} = k(\alpha_s)K_s^2 + k(\alpha_d)K_d^2 R_d + [\mu_B D_d(E_F)H_{hf,orb}]^2 R_{orb} \tag{2}$$

$$\alpha_s = I_s D_s(E_F) \qquad \alpha_d = I_d D_d(E_F). \tag{3}$$

In earlier work from our laboratory [2, 6, 7] it has been shown that a consistent interpretation of the NMR data for platinum catalysts can be obtained by considering only $D_s(E_F)$ and

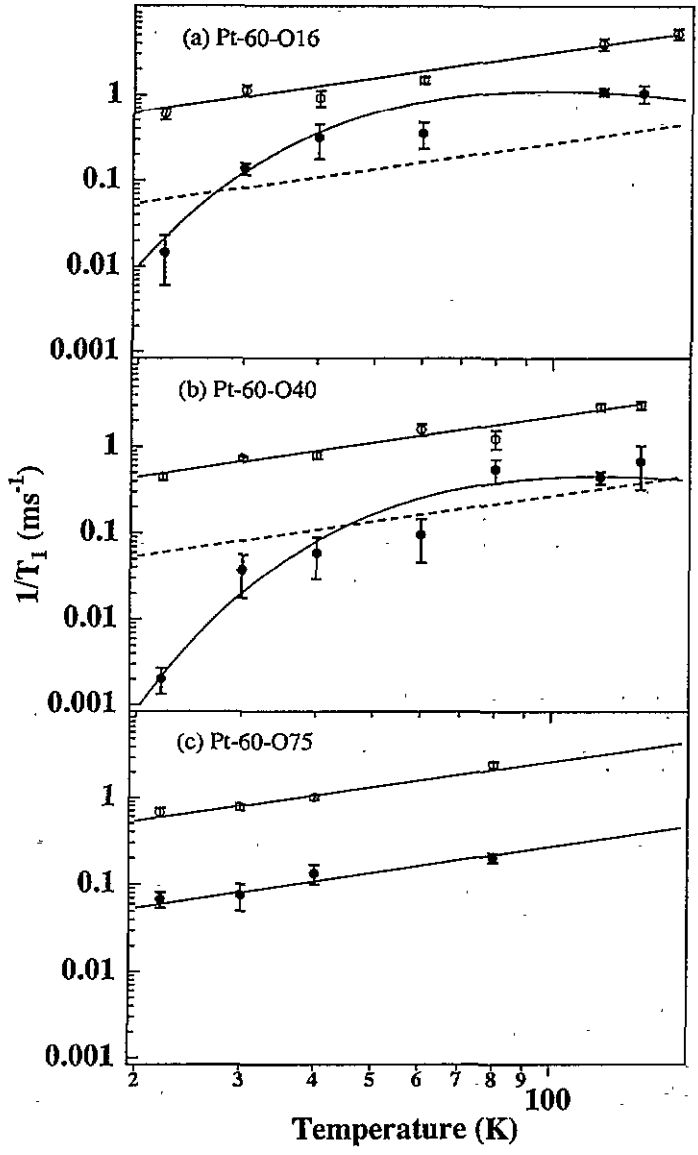

Figure 3. Variable-temperature spin–lattice relaxation data at fixed points in the spectra, fitted to double exponentials. In panels (a) to (c) respectively the amplitude ratios of the faster (open symbols) and lower (full symbols) exponentials are 1.3, 2.9 and 2.2, and the spectral positions are 1.098, 1.100 and 1.095 G kHz^{-1}. The straight lines indicate Korringa's law; the curves represent equation (6). The broken lines are for comparison with the slower relaxation in Pt-60-O75. The oxygen coverage is 0.16, 0.40 and 0.75 going from (a) to (c).

$D_d(E_F)$ as variables, and all other parameters in equations (1) and (2) as fixed (for the values adopted see table III in [2]). The meaning of these parameters is as follows: all H_{hf} are hyperfine fields (due to the spins of s-like electrons, of d-like electrons and to orbital effects); the two I's are exchange integrals; the two R's are reduction factors due to orbital degeneracy; χ_{orb} is the orbital susceptibility; and μ_B is the Bohr magneton. The functional

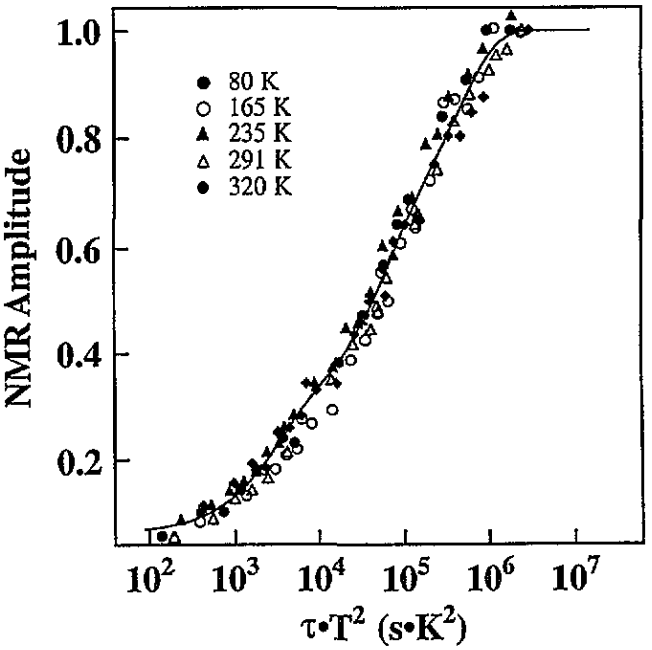

Figure 4. Time–temperature scaled nuclear spin–lattice relaxation curve at the maximum of the ^{195}Pt NMR spectrum (1.089 G kHz^{-1}) of α-PtO_2. The data fall on one (non-exponential) curve, suggesting that the elementary relaxation rates are proportional to T^2. Defining T_1^* as determining the 1/e point, one has T_1^* (320 K) = 0.14 s and T_1^* (80 K) = 2.26 s.

relationship $k(\alpha)$ between the Korringa enhancement factor k and the Stoner parameter α is taken to be the one proposed by Shaw and Warren [14]. The constant S is given by

$$S = (\gamma_e/\gamma_N)^2[\hbar/(4\pi k_B)] \tag{4}$$

where γ_e and γ_N are the electronic and nuclear gyromagnetic ratios and k_B is the Boltzmann constant. Its value for platinum is 5.59×10^{-6} s K. As an illustration, figure 5 gives a graphical solution of the two equations for a number of values of K and of $S(T_1T)^{-1}$.

For nuclei in a non-metallic state, we have been unable to identify clearly the mechanism of the non-Korringa relaxation observed in Pt-60-O16 and Pt-60-O40. In analogy to the situation in semiconductors, one might have expected that locally an energy gap E_g separates valence states from conduction states, and that the relaxation rates behaves as [15]

$$(T_1T)^{-1} = aT \exp(-E_g/2kT). \tag{5}$$

Here the factor T on the right-hand side comes from the hypothesis that the density of states in the conduction band is parabolic. At the same time, the shift of the NMR line should become temperature-dependent. Within our experimental precision, no temperature variation of the spectrum is found and the relaxation rate rather seems to follow the equation

$$T_1^{-1} = aT^{-2} \exp(-\Delta E/kT). \tag{6}$$

The fitted parameters a and $\Delta E/k$ are shown in table 1. In the intrinsic semiconductor tellurium, a contribution to the relaxation of the form of equation (6) has been ascribed to

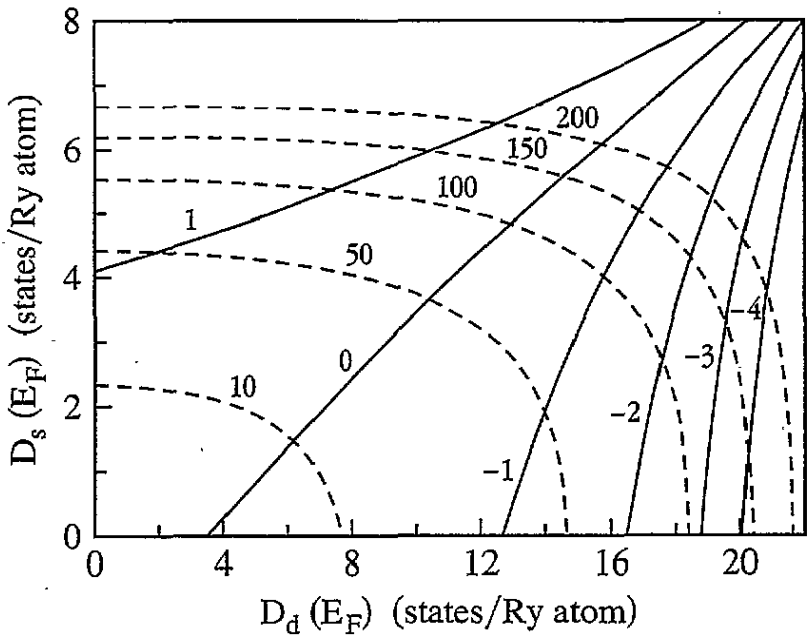

Figure 5. Contours of constant Knight shift K (%) (——) and of normalized relaxation rate S/T_1T (– – –), according to equations (1) and (2). A pair of experimental data (K, T_1) can be converted into a pair ($D_d(E_F)$, $D_s(E_F)$) by finding the intersection of the appropriate full and broken curves. Adapted from [3].

thermally created paramagnetic defects (vacancies) the diffuse slowly with respect to their electron-spin relaxation times, but rapidly on the NMR timescale [16]. In that case, the parameter ΔE represents the energy required to create the defect; we are not aware of any clue to the possible identity of such a defect in our samples. On the other hand, when we stick to the picture of a gap opening locally at the Fermi energy, the T^{-2} term may be due to a specific functional form of the local densities of states below and above the gap. If indeed the energy parameter found from the NMR curve is a local gap energy, its smallness would make it hard to detect by other techniques. For the same reason, it is not impossible that the temperature-dependent changes in the NMR spectrum, which should in principle be there, are too small to be detected.

Table 1. Some parameters of non-metallic NMR signals of Pt-60-O16 and Pt-60-O40 estimated from figures 2(a) and (b): θ represents the oxygen coverage (O/surface Pt); F gives the fraction of the non-Korringa NMR signal normalized by the dispersion of the sample (0.60); a and $\Delta E/k$ are the fitted parameters of equation (6).

θ	F	F/θ	a $\times 10^7$ (s^{-1} K^2)	$\Delta E/k$ (K)
0.16	0.43	2.7	4.7 ± 0.3	191 ± 6
0.40	0.58	1.5	7.9 ± 0.5	236 ± 9

5. Discussion

If the geometry of the particles remains unperturbed by the chemisorption, 60% of the area of the spectra is due to ^{195}Pt nuclei in the surface layer. The part of the spectrum ascribed to atoms in the interior of the particles (field/frequency ratio above 1.115 G kHz^{-1}) does not change significantly when going from Pt-60-clean to Pt-60-O16 to Pt-60-O40 and accounts for approximately 30% of all atoms. Therefore the non-metallic NMR signal in the two last samples must come (mainly) from surface sites. For convenience, we will consider in all four samples the spectral region up to 1.105 G kHz^{-1} as representative for the NMR behaviour of all surface nuclei. (This region actually contains 53% of the spectrum in Pt-60-clean, and 46, 53 and 61% when going from Pt-60-O16 to -O75). As remarked before, one would expect to observe temperature-dependent features in the spectrum when there is a gap in the local density of states at the Fermi energy. No such features have been detected in the available data (see figure 1). Since it is not easy to give a quantitative estimate of the expected effect, we cannot decide at the moment whether there is a real contradiction between experimental results and theoretical expectations.

It has been reported in the literature [10] that under some conditions oxygen selectively attacks the smaller particles in the sample. If this were the case here, one would expect the larger particles to have clean surfaces, so that a corresponding contribution to the relaxation curves should appear. Our double-exponential fits are of satisfactory quality without taking such a contribution into account: we find no evidence for selective chemisorption of oxygen on the smaller particles (but of course such fits cannot prove that the phenomenon does not exist).

There is a marked difference between the ^{195}Pt NMR spectra of our sample Pt-60-O75 and spectrum 3a in [8] of a SiO_2-supported passivated catalyst that has subsequently been exposed to air (here we will refer to that sample as Pt-59-air). Our sample has been exposed to oxygen for 120 h (although measurable uptake of oxygen only occurs very rapidly at the beginning of the exposure), but not to air, and does not show the PtO_2-like spectral feature near 1.089 G kHz^{-1} found in Pt-59-air. Rhodes *et al* [5] have also studied this question. When comparing their spectrum 8b of a surface freshly exposed to air after re-reduction (Pt-46-air) with our Pt-60-O75), one sees that initially the surface becomes mainly covered with oxygen. They conclude that the presence of hydrogen (or water) is necessary to obtain the so-called R-resonance, found after long exposure to air (shown in their spectrum 8a). This is confirmed by the differences in spectra between Pt-59-air and Pt-60-O75. The prolonged exposure of clean platinum particles to pure oxygen at room temperature does not lead to the formation of bulk-like oxides.

Certainly the most remarkable result is the metallic to non-metallic to metallic series of transitions locally observed for some surface sites as a function of oxygen coverage. (Similar series of bulk transitions as a function of composition are found in certain liquid binary alloys of free-electron-like metals; a well known bulk metal to non-metal transition as a function of oxide composition occurs in VO_x—see the references given in [17].) At the lowest coverage studied (0.16 atoms of oxygen per surface atom of platinum) approximately three non-metallic Pt sites are found for each oxygen atom; at a coverage of 0.40 this number is roughly halved and at 0.75 coverage it is zero (see table 1). It is interesting to compare these numbers with the value of one oxygen atom per four platinum atoms found as the saturation coverage on the Pt(111) surface under UHV conditions [18]. For a coverage of three oxygen atoms per four platinums, which is the saturation value under our experimental conditions, oxygen–oxygen direct bonding becomes important, and restores the metallic character of the underlying platinum surface. At the lower coverages, the oxygen–oxygen interaction is

mainly indirect, the platinum–oxygen interaction is rather localized, and the NMR properties of atoms in the deeper layers are essentially unaffected. However, the metallic surface sites have their LDOS modified by the presence of oxygen, as seen in figure 6. Contrary to the case of hydrogen chemisorption [6], where all surface sites obtain LDOS values smaller than or equal to those on the clean surface, the metallic surface sites in Pt-60-O16 and Pt-60-O40 have clearly enhanced values of LDOS. The average values in the spectral region of figure 6 are found to be 15.4, 21.7 and 18.7 states per rydberg per atom for Pt-60-clean, Pt-60-O16 and Pt-60-O40 respectively.

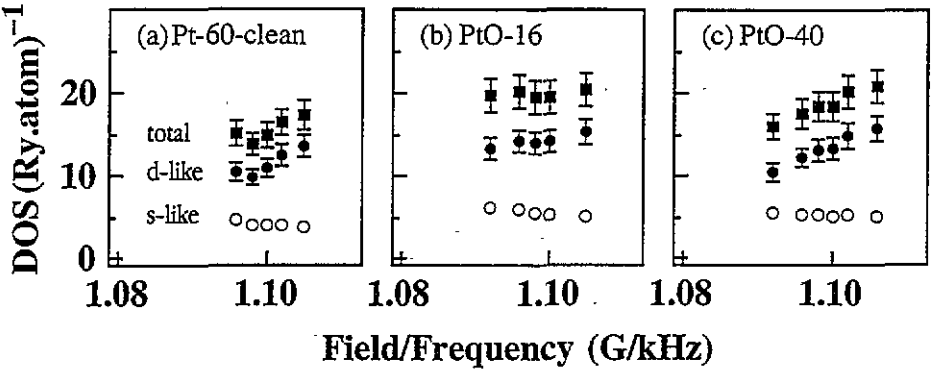

Figure 6. Local densities of state on metallic sites whose nuclei resonate in the surface region of the spectrum. For the clean surface, all surface nuclei are in a metallic environment; the amplitudes of the metallic signals in the surface region of Pt-60-O16 and Pt-60-O40 are given by the points in figures 2(a) and (b). The s-like and d-like densities of states plotted here are found from figures 2(d) and (e) (and from similar data for the clean surface, not shown) with the aid of equations (1) and (2).

This enhancement may be related to observed differences in the rate of chemisorption. In usual platinum catalysts, oxygen uptake is much more rapid than hydrogen uptake: oxygen adsorption is completed below 1 Torr while the isotherm of hydrogen adsorption joins the horizontal asymptote above 100 Torr [19]. As mentioned in section 1, the electron density at the Fermi energy on surface sites probably is important for the response of the surface to an incoming reactant. According to the NMR data, after some initial oxygen chemisorption, the LDOS on 'unoccupied' surface sites increases, thereby increasing the reactivity of these sites; for hydrogen chemisorption this does not occur (and probably even the opposite happens, since no sites are found with an increased LDOS). Another connection may be with the observation that (under UHV conditions) adsorbed CO inhibits the dissociative adsorption of oxygen, but adsorbed oxygen does not inhibit molecular CO adsorption [20]. Available ^{195}Pt NMR data indicate that the effect of CO on the surface LDOS is similar to that of hydrogen [21]: therefore pre-adsorption of CO would be expected to diminish (or at least not to improve) the reactivity of the rest of the surface, whereas pre-adsorption of oxygen would increase it.

Instead of considering only the metallic sites within the surface region of the spectrum, we may also calculate the average LDOS over all of the surface signal (the part of the spectrum below 1.105 G kHz^{-1}), setting the LDOS at non-metallic sites equal to zero. Then we find that values given in table 2. They hardly change with oxygen coverage. Such averages play a role when chemisorption is studied by magnetic susceptibility experiments: the results of table 2 predict that the effect of oxygen chemisorption will be small.

Table 2. Average local densities of states over all sites (metallic and non-metallic) in the surface region of the spectrum (defined as $H/\nu_0 \leqslant 1.105$ G kHz^{-1}). For Pt-60-O16 and Pt-60-O40 the difference signal between the full lines and the points in figures 2(a) and (b) is taken as corresponding to zero-LDOS sites. For Pt-60-O75 both relaxation rates in figure 2(f) correspond to metallic sites and the average in this table corresponds to a weighting with the amplitudes in figure 2(c).

	NMR amplitude-weighted surface-like LDOS ((Ryd atom)$^{-1}$)		
Sample	s-like	d-like	total
Pt-60-clean	4.16	11.26	15.4
Pt-60-O16	3.94	9.98	13.9
Pt-60-O40	3.91	10.07	14.0
Pt-60-O75	4.73	11.28	15.9

6. Conclusion

In this paper, the temperature dependence of the ^{195}Pt nuclear spin–lattice relaxation rate T_1^{-1} in the surface region of the NMR spectrum has been studied as a function of temperature T, for four different oxygen dosings (coverages θ of 0, 0.16, 0.40 and 0.75). For the two intermediate coverages (0.16 and 0.40) a part of the surface NMR signal does not relax according to the T_1T = constant law normally found for metals. This is a qualitative demonstration that (for $\theta = 0.16$ and 0.40) part of the surface Pt atoms are not in a metallic environment. From fits to the relaxation curves we find that at $\theta = 0.16$ there are approximately 2.7 non-metallic Pt atoms per oxygen atom; for $\theta = 0.40$ this number is 1.5; while at $\theta = 0$ and $\theta = 0.75$ all surface sites are metallic. A qualitative comparison of the temperature dependences of T_1^{-1} shows that the non-metallic atoms are not in a α-PtO_2-like environment.

From fits of the relaxation curves, and using the relations between local densities of state (LDOS) at the Fermi energy on the one hand, and the Knight shift and relaxation rates on the other, we obtain average values for the s-like and d-like LDOS on the metallic surface sites. Similar analyses of NMR data have been made previously for Pt catalysts with hydrogen-covered surfaces, where it was found that the LDOS values decrease with respect to the clean surface [6]. In contrast to this, the metallic sites on oxygen-covered surfaces have an enhanced LDOS. Using the correlation between the density of Fermi-level electrons at the surface and the reactivity, these differences in LDOS behaviour can be related to differences in chemisorption behaviour.

Acknowledgments

We thank I Rodicio and M Graetzel for providing the starting material for the samples. This research was supported by the Swiss National Science Foundation (Grant 21-31127.91).

References

[1] Hoffman R 1988 *Rev. Mod. Phys.* **60** 601
[2] Bucher J P and van der Klink J J 1988 *Phys. Rev.* B **38** 11 038
[3] Yafet Y and Jaccarino V 1964 *Phys. Rev.* **133** A1630

[4] Jaccarino V 1965 *Nuclear Magnetic Resonance and Relaxation in Solids* ed L Van Gerven (Amsterdam: North-Holland) and references therein
[5] Rhodes H E, Wang P K, Stokes H T, Slichter C P and Sinfelt J H 1982 *Phys. Rev.* B **26** 3559
[6] Tong Y Y and van der Klink J J 1994 *J. Phys. Chem.* **98** 11 011
[7] Tong Y Y, Martin G A and van der Klink J J 1994 *J. Phys.: Condens. Matter* **6** L533
[8] Bucher J P, Buttet J, van der Klink J J and Graetzel M 1989 *Surf. Sci.* **214** 347
[9] Bucher J P, van der Klink J J and Graetzel M 1990 *J. Phys. Chem.* **94** 1209
[10] Gnutzmann V and Vogel W 1990 *J. Phys. Chem.* **94** 4991
[11] McBride J R, Graham G W, Peters C R and Weber W H 1991 *J. Appl. Phys.* **69** 1596
[12] Otto K, Weber W H, Graham G W and Shyu J Z 1989 *Appl. Surf. Sci.* **37** 250
[13] Levitt M H 1982 *J. Magn. Reson.* **48** 234
[14] Shaw R W Jr and Warren W W Jr 1971 *Phys. Rev.* B **3** 1562
[15] Bloembergen N 1954 *Physica* **20** 1130
[16] Kanert O 1982 *Phys. Rep.* **91** 183
[17] Edwards P P and Rao C N R (ed) 1985 *The Metallic and Non-Metallic States of Matter* (London: Taylor and Francis)
[18] Luntz A G, Williams M D and Bethune D S 1988 *J. Chem. Phys.* **89** 4381
[19] Candy J P, Fouilloux P and Renouprez A J 1980 *J. Chem. Soc., Faraday Trans. I* **76** 616
[20] Gland J L and Kollin E B 1983 *J. Chem. Phys.* **78** 963
[21] Ansermet J P 1985 *PhD Thesis* University of Illinois, cited in [2]